Systematic Review and Meta-Analysis

Medicine®

OPEN

Bioinformatic analysis of the pathogenic mechanism of talaromyces marneffei infection

Jiemei Cen, MS[a,b], Jiarui Chen, MS[c], Ye Qiu, MD[b], Wen Zeng, MD[b], Jianquan Zhang, MD[a,*]

Abstract

Background: Talaromyces marneffei (T marneffei), known as a significant pathogen in patients with AIDS in Southeast Asia, is a dimorphic fungus, which can cause deadly systematic infection in immunocompromised hosts. What is more, the dimorphic phase transition has been reported as a conspicuous process linked with virulence. Interestingly, the yeast form was found in infected individuals, representing the pathogenic phase. However, few researches were found to study the mechanism of dimorphic transition. Thus, a diverse insight into the dimorphic switch mechanism, is urgently needed and we are the first one to research the mechanism of dimorphism.

Methods: Firstly, we investigated the microarray of T. marneffei in the Gene Expression Omnibus database (GEO) for differentially expressed genes (DEGs). Then Database for Annotation, Visualization and Integrated Discovery (DAVID) v6.8 was employed to analyze the underlying enrichment and pathway in biological process of DEGs. Meanwhile, protein-protein interaction (PPI) network was constructed using STRING database. On the strength of the theory that similar amino acid sequences share similar structures, which play a decisive role on the function of protein, three dimensional structures of hub-genes were predicted to further investigate the likely function of hub-genes.

Results: GSE51109 was elected as the eligible series for the purpose of our research, including GSM1238923 (GSM23), GSM1238924 (GSM24), and GSM1238925 (GSM25). PMAA_012920, PMAA_028730, PMAA_068140, PMAA_092900, PMAA_032350 were the most remarkable genes in all of the three PPI networks, thus, were viewed as hub-genes. With regard to the three-dimensional construction, except that there was no significant prediction structure of PMAA_092900 with the criterion seq identify $>30\%$, GMQE: 0-1, QMEAN4: -4-0, the parallel templates for four structures were Crystal structure of Saccharomyces cerevesiae mitochondrial NADP(+)-dependent isocitrate dehydrogenase in complex with isocitrate, Organellar two-pore channels (TPCs), Yeast Isocitrate Dehydrogenase (Apo Form) and Crystal Structure Of ATP-Dependent Phosphoenolpyruvate Carboxykinase From Thermus thermophilus HB8 in order.

Conclusion: The dimorphic transition of T. marneffei was viewed as a pathogenic factor and DEGs were observed. In-depth study of the function and pathway of DEGs revealed that PMAA_012920, PMAA_028730, PMAA_068140, PMAA_092900, PMAA_032350 were most likely acting as the hub-genes and were likely taking effect through regulating energy metabolism.

Abbreviations: BP = Biological Process, CC = Cellular Component, DEG = differentially expressed gene, GEO = gene expression omnibus, GO = gene ontology, GSM23 = GSM1238923, GSM24 = GSM1238924, GSM25 = GSM1238925, KEGG = Kyoto Encyclopedia of Genes and Genomes, MF = molecular function, PPI = protein–protein interaction, T.marneffei = Talaromyces marneffei.

Keywords: bioinformatic analysis, dimorphic transition, pathogenic mechanism, talaromyces marneffei

Editor: Muhammad Tarek Abdel Ghafar.

JC and JC have contributed to the work equally and should be regarded as co-first authors.

This article does not contain any studies with human participants or animals performed by any of the authors.

This article does not contain any studies with human participants performed by any of the authors.

The dataset used and/or analyzed during the current study are available from the corresponding author on reasonable request.

This work was supported by the Natural Science Foundation of China [grant numbers NSFC81760010 and 82060364].

The authors declare that they have no conflicts of interest in association with this study.

The datasets generated during and/or analyzed during the current study are publicly available.

[a] *Department of Respiratory Medicine, the Eighth Affiliated Hospital, Sun Yat-sen University, Shenzhen, Guangdong,* [b] *Department of Respiratory Medicine,* [c] *Spine and Osteopathy Ward, The First Affiliated Hospital of Guangxi Medical University, Nanning, Guangxi, China.*

[*] *Correspondence: Jianquan Zhang, Department of Respiratory Medicine, the Eighth Affiliated Hospital, Sun Yat-Sen University, Shenzhen, Guangdong, People's Republic of China, No. 3025, Shennan Middle Road, Futian District, Shenzhen, Guangdong 518033, People's Republic of China (e-mail: jqzhang2002@126.com).*

How to cite this article: Cen J, Chen J, Qiu Y, Zeng W, Zhang J. Bioinformatic analysis of the pathogenic mechanism of talaromyces marneffei infection. Medicine 2020;99:48(e23409).

Received: 27 March 2020 / Received in final form: 26 October 2020 / Accepted: 29 October 2020

http://dx.doi.org/10.1097/MD.0000000000023409

1. Introduction

T marneffei, previously known as Penicillium marneffei, was a crucial opportunistic thermal dimorphic fungus most prevalent in Southeast Asia[1] that cause systematic mycosis, such as lung infection, bone invasion, and skin lesion. Still, there are some cases reported as ecdemic cases. Bamboo rats were accepted as host species of T marneffei, and the soil of their burrows was a source of T marneffei as well. Once infected, it can be an intractable case and is life threatening and require long-term treatment, which is costly. Over the years, an increasing number of cases occurred in immunocompetent patients have been reported, thus increased social and family burden. Phase switch, known as a factor linked with virulence, that is to say, it can grow into a multicellular hyphal form at 25°C while a unicellular fission yeast form at 37°C. In addition, in response to specific temperature cues, the hyphal form can undergo asexual development (conidiation) and produce a differentiated multicellular structure called conidiophore which produces dormant spores (conidia) and inhaled conidia initiates infection and only the yeast form was found in infected individuals. Should there be a specific agent that can inhibit the binary conversion of talaromyces marneffei, less people will suffer from infection. Therefore, in this research, we pay attention to the genes of talromyces marneffei closely related to dimorphism transmission, which play a key role in pathogenicity, anticipating to reveal the key factors of virulence and further explore the characteristic of them, which may contribute to find the precise agent to inhibit the growth of this fungus.

Since the 1980s, when the first case of T marneffei infection was reported, virulence has been a fierce debate and some researches have been executed to investigate the toxicity of T marneffei.[2] The phase switch, viewed as an indispensable element for virulence, the molecular mechanism of which was still unclear. Therefore, the investigations of the molecular changes are pressed for. There have been an accumulating amount of researches regarding to pathogenic mechanism of other disease, such as breast cancer and myeloid leukemia through bioinformatic tools, taking single-cell genomics, RNA sequencing, transcriptomics,[3,4] proteomics[5] and time resolved quantitative phospho-tyrosine analysis[6] as samples, and found certain molecule to be crucial in disease progression and prognosis. Thus, bioinformatic tools were implied to research the differentially expressed genes during dimorphic switch of talaromyces marneffei and expected that some key genes would be found to be crucial in pathogenic mechanism of T marneffei infection.

2. Materials and methods

2.1. Differentially expressed genes acquisition

The gene expression profile GSE51109, deposited by Pasricha et al,[7] was downloaded from GEO database (https://www.ncbi.nlm.nih.gov/geo/). Based on the platform of the GPL17756 [Pm 5K Random Array I] Affymetrix Human Genome U133 Plus 2.0 Array, the gene expression profile contained three samples, including the genes expression with respect to intercomparing among hyphal form, yeast form and conidia. PCR products from previously cloned Penicillium marneffei genes with known expression profiles were included as controls on the microarray. Data were normalized using a global loess curve for each array[8] and given normalized log2 ratio ch2/ch1 representing pair-wise combinations. Genes with log FC absolute value no less than 1 were selected as DEGs.

2.2. GO enrichment analysis and pathway analysis

Since the DEGs were screened out, the biological function and enrichment pathways of DEGs were further investigated by DAVID v6.8 (https://david.ncifcrf.gov/home.jsp), which greatly contributes to understanding biological meaning behind large list of genes by providing a comprehensive set of tools for investigators. As a consequence, several functions can be conducted with regard to the submitted gene lists, for example, identified enriched biological themes, particularly Gene Ontology (GO) terms, discover enriched functional-related gene groups, visualize genes on BioCarta & Kyoto Encyclopedia of Genes and Genomes (KEGG) pathway maps, search for other functionally related genes not in the list, list interacting proteins and so on. Therefore, to better understand the potential function of DEGs, DAVIDv6.8 was employed to analyze the underlying enrichment and pathway in biological process of DEGs.

2.3. Protein-protein interaction (PPI) network construction

As is known to us all, genes taking effect were influenced by series factors such as other genes and other micro molecule. Aiming to explore the specific relationship between DEGs, we constructed a network displaying the interaction between DEGs by STRING (https://string-db.org/cgi/about.pl?footer_active_subpage=content), a database which contains known and predicted protein-protein interaction, including direct (physical) and indirect (functional) associations. The interaction sources are based on computational prediction, knowledge transfer between organisms, and interactions aggregated from other databases. Genomic Context Predictions, High-throughput Lab Experiments, (Conserved) Co-Expression, Automated Text mining, Previous Knowledge in Databases make up the five main sources that give support to the interaction. To gain a deeper insight into the molecular mechanism of pathogenicity, the DEGs were uploaded to STRING then export the image of PPI and the top five most connected nodes were selected as hub-genes.

2.4. Protein three-dimensional structure construction

Genes give play to regulate the biological function or produce certain protein after transcription and translation. Thus, we were committed to predict the protein of each hub-genes through constructing the protein three-dimensional structure of each hub-genes. Accessible via the ExPASy web server, or from the program DeepView (Swiss Pdb-Viewer), SWISS-MODEL is a fully automated protein structure homology-modelling server, with the purpose of making protein modelling accessible to all life science researchers worldwide.[9] Regarding to that the hub-genes were elected, further investigation into the specific functions of these genes is necessary. On the strength of the theory that similar amino acid sequences share similar structures, which play a decisive role on the function of protein, each hub-gene's nucleotide sequence downloaded from National Center for Biotechnology Information Search database(NCBI) were submitted to NovoPro (http://www.novopro.cn/tools/translate.html) database for translation, then SWISS-MODEL was exploited for the protein three-dimensional structure construction. Afterwards, the elected templates were uploaded to RCSB-PDB

Table 1

The result of GO and pathway analysis of GSM23.

Category	Term	Count	%	*P* value	Genes
GOTERM_BP	generation of precursor metabolites and energy	6	3.09278	.007248	PMAA_039680, PMAA_028880, PMAA_046420, PMAA_068140, PMAA_089220, PMAA_071630
GOTERM_BP	inorganic cation transmembrane transport	4	2.06186	.020237	PMAA_040300, PMAA_042510, PMAA_010280, PMAA_041270
GOTERM_BP	inorganic ion transmembrane transport	4	2.06186	.020237	PMAA_040300, PMAA_042510, PMAA_010280, PMAA_041270
GOTERM_BP	cation transmembrane transport	4	2.06186	.021917	PMAA_040300, PMAA_042510, PMAA_010280, PMAA_041270
GOTERM_BP	ion transmembrane transport	4	2.06186	.031433	PMAA_040300, PMAA_042510, PMAA_010280, PMAA_041270
GOTERM_CC	mitochondrion	18	9.27835	2.57E-04	PMAA_073320, PMAA_094650, PMAA_055980, PMAA_067490, PMAA_060200, PMAA_098380, PMAA_038320, PMAA_068140, PMAA_041520, PMAA_005360, PMAA_071070, PMAA_024900, PMAA_046420, PMAA_020160, PMAA_089220, PMAA_092720, PMAA_028730, PMAA_040640
GOTERM_CC	cytoplasm	42	21.6495	.014158	PMAA_037440, PMAA_013400, PMAA_092900, PMAA_094610, PMAA_047150, PMAA_020080, PMAA_094650, PMAA_067490, PMAA_060200, PMAA_041840, PMAA_068140, PMAA_038320, PMAA_005360, PMAA_045500, PMAA_071690, PMAA_071070, PMAA_040300, PMAA_057320, PMAA_024900, PMAA_020160, PMAA_006690, PMAA_089220, PMAA_092720, PMAA_069820, PMAA_039810, PMAA_073320, PMAA_041270, PMAA_055980, PMAA_098380, PMAA_004490, PMAA_016130, PMAA_032350, PMAA_041520, PMAA_010280, PMAA_042510, PMAA_099880, PMAA_046420, PMAA_039640, PMAA_011350, PMAA_028730, PMAA_040640, PMAA_019030
GOTERM_CC	cytoplasmic part	38	19.5876	.01651	PMAA_037440, PMAA_013400, PMAA_094610, PMAA_047150, PMAA_094650, PMAA_067490, PMAA_060200, PMAA_041840, PMAA_068140, PMAA_038320, PMAA_005360, PMAA_045500, PMAA_071690, PMAA_071070, PMAA_040300, PMAA_057320, PMAA_024900, PMAA_020160, PMAA_006690, PMAA_089220, PMAA_092720, PMAA_039810, PMAA_073320, PMAA_041270, PMAA_055980, PMAA_098380, PMAA_004490, PMAA_016130, PMAA_032350, PMAA_041520, PMAA_010280, PMAA_042510, PMAA_099880, PMAA_046420, PMAA_011350, PMAA_028730, PMAA_040640, PMAA_019030
GOTERM_MF	oxidoreductase activity	39	20.1031	1.24E-04	PMAA_065440, PMAA_092900, PMAA_030170, PMAA_032300, PMAA_022690, PMAA_068140, PMAA_065580, PMAA_042280, PMAA_079980, PMAA_027680, PMAA_012920, PMAA_039120, PMAA_043060, PMAA_082030, PMAA_071760, PMAA_020160, PMAA_029890, PMAA_021820, PMAA_088690, PMAA_089220, PMAA_089910, PMAA_075640, PMAA_021280, PMAA_097070, PMAA_064620, PMAA_098380, PMAA_064600, PMAA_073270, PMAA_071630, PMAA_024760, PMAA_028330, PMAA_039680, PMAA_093480, PMAA_046420, PMAA_015980, PMAA_028730, PMAA_066300, PMAA_065540, PMAA_100150
GOTERM_MF	catalytic activity	99	51.0309	.001285	PMAA_065440, PMAA_094610, PMAA_002930, PMAA_080980, PMAA_065580, PMAA_023440, PMAA_042500, PMAA_081090, PMAA_071690, PMAA_094890, PMAA_092640, PMAA_082030, PMAA_006690, PMAA_088690, PMAA_089220, PMAA_069820, PMAA_101020, PMAA_075640, PMAA_028880, PMAA_097070, PMAA_091380,

(*continued*)

Table 1
(continued).

Category	Term	Count	%	*P* value	Genes
					PMAA_064990, PMAA_032350, PMAA_016130, PMAA_059640, PMAA_036000, PMAA_082040, PMAA_080560, PMAA_019030, PMAA_082600, PMAA_030170, PMAA_007900, PMAA_068140, PMAA_042280, PMAA_095670, PMAA_040300, PMAA_093350, PMAA_071760, PMAA_029890, PMAA_002470, PMAA_021280, PMAA_060900, PMAA_073270, PMAA_071630, PMAA_024760, PMAA_040070, PMAA_093480, PMAA_066300, PMAA_100150, PMAA_037440, PMAA_013400, PMAA_092900, PMAA_076130, PMAA_086380, PMAA_094650, PMAA_067490, PMAA_041840, PMAA_079980, PMAA_045500, PMAA_071070, PMAA_012920, PMAA_043060, PMAA_015360, PMAA_020160, PMAA_082620, PMAA_010220, PMAA_089910, PMAA_039810, PMAA_054650, PMAA_081560, PMAA_055590, PMAA_064600, PMAA_079710, PMAA_065680, PMAA_052600, PMAA_039680, PMAA_028730, PMAA_015980, PMAA_032300, PMAA_014300, PMAA_022690, PMAA_020080, PMAA_002910, PMAA_027680, PMAA_091840, PMAA_093910, PMAA_039120, PMAA_063790, PMAA_021820, PMAA_092720, PMAA_092050, PMAA_064620

database for relevant literatures about the eligible templates. As a result, the function of the protein, into which hub-genes translated can be duplicated from the templates.

3. Results

3.1. Differentially expressed genes acquisition

According to the obtained GEO series GSE51109, there are a total of 194, 169 and 157 DEGs for GSM23, GSM24 and GSM25 respectively, among which, up-regulation genes for each is 115, 98 and 80, while down-regulation genes account for 79, 71, and 77 severally.

3.2. GO enrichment analysis and pathway analysis

As is shown in Tables 1 to 3, GO enrichment was composed of biological process (BP), cellular component(CC) and molecular function(MF), taking the *P* value of $<.05$ as a significant criteria, the top five items of BP, CC and MF were extracted and when the significant items less than 5, all of the actual significant items were shown. In Table 1, the result of GO enrichment and pathway analysis of GSM23, namely conidiation versus hyphal cell types, were listed. As for BP, the top five items were generation of precursor metabolites and energy, inorganic cation transmembrane transport, inorganic ion transmembrane transport, cation transmembrane transport, ion transmembrane transport. While mitochondrion, cytoplasm and cytoplasmic part were the only three significant items about CC. For MF, oxidoreductase activity, catalytic activity, isocitrate dehydrogenase activity, NAD binding, oxidoreductase activity, acting on the aldehyde or oxo group of donors were significant results in response to the given criterion. In our research, no significant result was seen in pathway. As to GSM24, shown in Table 2, organic acid metabolic process, generation of precursor metabolites and energy, organonitrogen compound metabolic process, small molecule metabolic process, single-organism metabolic process were the top five BP stuffs. As regard to MF, isocitrate dehydrogenase activity, oxidoreductase activity, NAD binding, magnesium ion binding, cofactor binding was the top five results, while there was no result for CC and pathway analysis. The enrichment and pathway analysis results of GSM25 were displayed in Table 3, from which, we can obtain the outcome that organic acid metabolic process, membrane, dioxygenase activity, oxidoreductase activity represented for the top five items of BP, CC, MF respectively. As the same, no pathway was enriched in for the DEGs of GSM25.

3.3. PPI network construction

The aforementioned 194, 169 and 157 DEGs for GSM23, GSM24 and GSM25 were submitted to the STRING database to uncover the potential protein-protein interactions so as to get a better understanding of the potential molecular mechanism. As is shown in Figures 1 to 3, the PPI networks were constructed in response to the DEGs of GSM23, GSM24, GSM25 with the confidence score $>$ 0.4. According to the networks, we observed that the connections among the following genes: PMAA_012920, PMAA_028730, PMAA_068140, PMAA_092900, PMAA_032350 were the most remarkable in all of the 3 networks. The results implied that those genes may be the key genes in dimorphic transition. Furthermore, as is said by picture 4, the three-dimensional structures of proteins which these genes translated into remained unclear.

3.4. Protein three-dimensional structure construction

Based on the prevalent theory that semblable structure was related with similar function referring to protein, the three-

Table 2

The result of GO and pathway analysis of GSM24.

Category	Term	Count	%	*P* value	Genes
OTERM_BP	organic acid metabolic process	16	9.467456	5.28E-04	PMAA_080350, PMAA_069820, PMAA_005580, PMAA_028880, PMAA_097060, PMAA_068140, PMAA_046930, PMAA_012920, PMAA_013650, PMAA_005610, PMAA_039680, PMAA_031950, PMAA_046420, PMAA_089220, PMAA_028730, PMAA_041990
GOTERM_BP	generation of precursor metabolites and energy	7	4.142012	.001382	PMAA_039680, PMAA_028880, PMAA_046420, PMAA_005310, PMAA_068140, PMAA_089220, PMAA_071630
GOTERM_BP	organonitrogen compound metabolic process	24	14.20118	.001518	PMAA_080350, PMAA_024190, PMAA_028110, PMAA_102650, PMAA_073320, PMAA_047150, PMAA_032300, PMAA_028880, PMAA_002470, PMAA_097060, PMAA_086380, PMAA_005310, PMAA_026340, PMAA_055500, PMAA_073270, PMAA_046930, PMAA_013650, PMAA_005610, PMAA_039680, PMAA_031950, PMAA_054240, PMAA_092720, PMAA_028730, PMAA_041990
GOTERM_BP	small molecule metabolic process	21	12.42604	.001884	PMAA_080350, PMAA_069820, PMAA_102650, PMAA_005580, PMAA_028880, PMAA_002470, PMAA_097060, PMAA_086380, PMAA_005310, PMAA_068140, PMAA_073270, PMAA_046930, PMAA_012920, PMAA_013650, PMAA_005610, PMAA_039680, PMAA_031950, PMAA_046420, PMAA_089220, PMAA_028730, PMAA_041990
GOTERM_BP	single-organism metabolic process	27	15.97633	.003027	PMAA_005580, PMAA_102650, PMAA_053530, PMAA_032300, PMAA_097060, PMAA_086380, PMAA_068140, PMAA_046930, PMAA_081090, PMAA_012920, PMAA_013650, PMAA_038970, PMAA_031950, PMAA_089220, PMAA_080350, PMAA_069820, PMAA_028880, PMAA_002470, PMAA_005310, PMAA_073270, PMAA_071630, PMAA_005610, PMAA_039680, PMAA_046420, PMAA_037600, PMAA_041990, PMAA_028730
GOTERM_MF	isocitrate dehydrogenase activity	3	1.775148	.001362	PMAA_012920, PMAA_046420, PMAA_068140
GOTERM_MF	oxidoreductase activity	30	17.75148	.011744	PMAA_024520, PMAA_017780, PMAA_032300, PMAA_065580, PMAA_068140, PMAA_042280, PMAA_079980, PMAA_057450, PMAA_018640, PMAA_027680, PMAA_012920, PMAA_043060, PMAA_031950, PMAA_071760, PMAA_029890, PMAA_088690, PMAA_089220, PMAA_097070, PMAA_098380, PMAA_064600, PMAA_073270, PMAA_071630, PMAA_075990, PMAA_005610, PMAA_039680, PMAA_046420, PMAA_028730, PMAA_065540, PMAA_022840, PMAA_100150
GOTERM_MF	NAD binding	5	2.95858	.017914	PMAA_012920, PMAA_039680, PMAA_046420, PMAA_068140, PMAA_065540
GOTERM_MF	magnesium ion binding	5	2.95858	.020596	PMAA_035040, PMAA_012920, PMAA_005580, PMAA_046420, PMAA_068140
GOTERM_MF	cofactor binding	14	8.284024	.038482	PMAA_035040, PMAA_097060, PMAA_055590, PMAA_068140, PMAA_042280, PMAA_073270, PMAA_079980, PMAA_065680, PMAA_012920, PMAA_041410, PMAA_039680, PMAA_046420, PMAA_035660, PMAA_065540

dimensional structures of the five hub-genes were constructed, which were shown in Figures 4 to 7. Nevertheless, there was no significant prediction structure of the hug-gene PMAA_092900 with the criterion seq identify >30%, GMQE: 0–1, QMEAN4: -4–0. Then the rest four significant predicted structures were confronted with the examination of the following tools: verify 3D, Procheck, Whatcheck, Errat and Prove, luckily, the above-mentioned four structures were qualified since they met the criteria of at least three inspection tools. When consult to the PDB database for the specific function of templates, representing the function of the predicted protein, the parallel templates for four structures were Crystal structure of Saccharomyces cerevesiae mitochondrial nicotinamide adenine dinucleotide phosphate (NADP)(+)-dependent isocitrate dehydrogenase in complex with

Table 3

The result of GO and pathway analysis of GSM25.

Category	Term	Count	%	*P* value	Genes
GOTERM_BP	organic acid metabolic process	9	5.769230769	.0458589	PMAA_069820, PMAA_046930, PMAA_005610, PMAA_005580, PMAA_013650, PMAA_031950, PMAA_089220, PMAA_028730, PMAA_040640
GOTERM_CC	membrane	38	24.35897436	.0497946	PMAA_024520, PMAA_017430, PMAA_078940, PMAA_045900, PMAA_100870, PMAA_032300, PMAA_044710, PMAA_038320, PMAA_018640, PMAA_057450, PMAA_040300, PMAA_035260, PMAA_094330, PMAA_058480, PMAA_006690, PMAA_021820, PMAA_072760, PMAA_089220, PMAA_088670, PMAA_047000, PMAA_039850, PMAA_101530, PMAA_057360, PMAA_056120, PMAA_065470, PMAA_041270, PMAA_091940, PMAA_045600, PMAA_004490, PMAA_049550, PMAA_041520, PMAA_037620, PMAA_078310, PMAA_027500, PMAA_074850, PMAA_059270, PMAA_049040, PMAA_019030
GOTERM_MF	dioxygenase activity	5	3.205128205	.0065975	PMAA_024760, PMAA_075640, PMAA_021280, PMAA_031950, PMAA_097070
GOTERM_MF	oxidoreductase activity	24	15.38461538	.019369	PMAA_024520, PMAA_027300, PMAA_075640, PMAA_032300, PMAA_021280, PMAA_022690, PMAA_064620, PMAA_097070, PMAA_065580, PMAA_057450, PMAA_018640, PMAA_024760, PMAA_075990, PMAA_005610, PMAA_039120, PMAA_031950, PMAA_082030, PMAA_093480, PMAA_021820, PMAA_089220, PMAA_066300, PMAA_028730, PMAA_022840, PMAA_100150

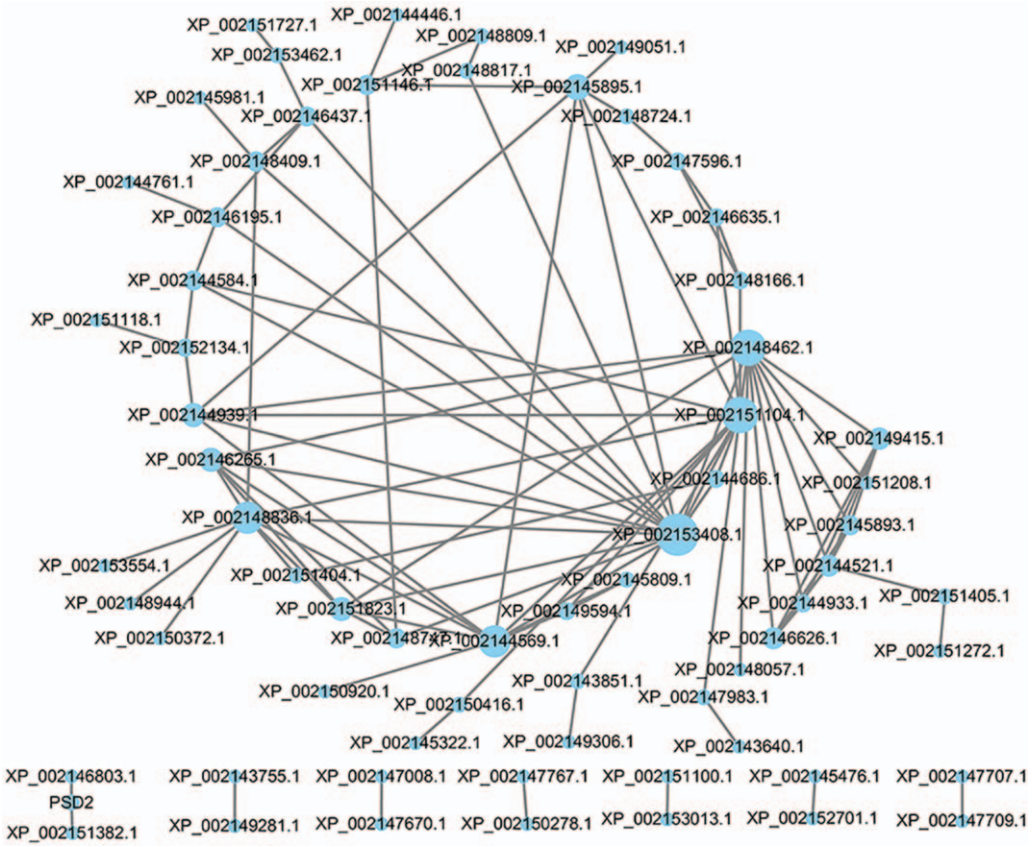

Figure 1. PPI network of GSM23. XP002153408.1, XP002144569.1, XP002146265.1, XP002148836.1 and XP002144939.1 represent the gene of PMAA-012920, PMAA-028730, PMAA-068140, PMAA-0092900 and PMAA-032350 respectively. The size of nodes range according to the degree of analysis.

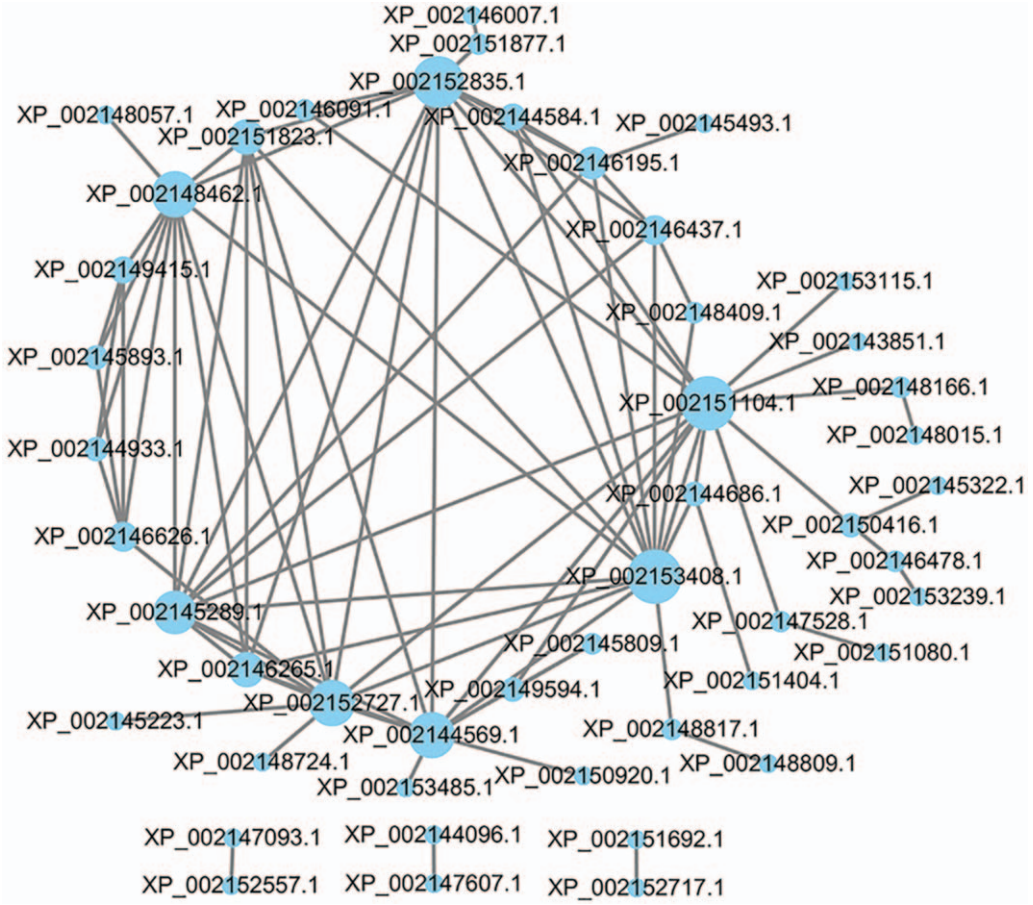

Figure 2. GSM24. XP002153408.1, XP002144569.1, XP002146265.1, XP002148836.1 and XP002144939.1 represent the gene of PMAA-012920, PMAA-028730, PMAA-068140, PMAA-0092900 and PMAA-032350 respectively. The size of nodes range according to the degree of analysis.

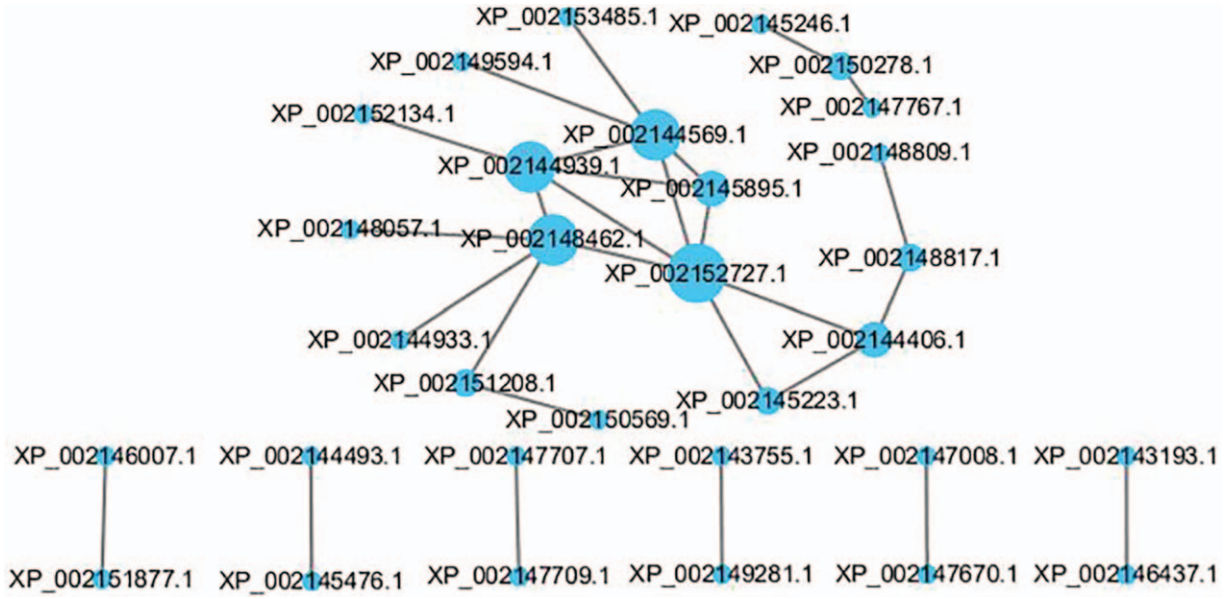

Figure 3. GSM25. XP002153408.1, XP002144569.1, XP002146265.1, XP002148836.1 and XP002144939.1 represent the gene of PMAA-012920, PMAA-028730, PMAA-068140, PMAA-0092900 and PMAA-032350 respectively. The size of nodes range according to the degree of analysis.

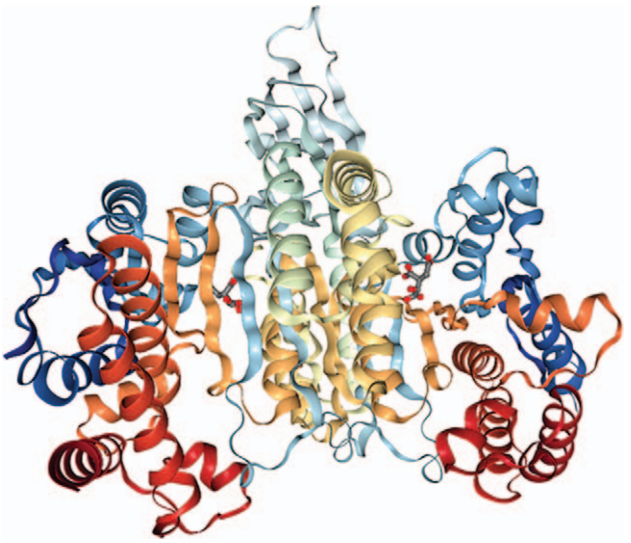

Figure 4. The predicted three-dimensional structure of PMAA-012920.

isocitrate, Organellar two-pore channels (TPCs), Yeast Isocitrate Dehydrogenase (Apo Form) and Crystal Structure Of ATP-Dependent Phosphoenolpyruvate Carboxykinase From Thermus thermophilus HB8 in order.

3.5. Validation of DEGs and hub-genes

GSE51109 contains data about the comparisons between three phases, from which, we extracted DEGs and hub-genes and found that PMAA_068140, PMAA_012920, PMAA_028730, PMAA_092900, PMAA_032350 were obviously differentially expressed and connected with other genes widely. In order to further verify whether their expressions were different indeed in these fungal biological states or transformation processes, we downloaded GSE51110 from the GEO database. GSE51110 gave a deep insight into the DEGs between dimorphism transition by comparing the different expression profile between hyphal cells and after transferring to 37°C as well as yeast cells and yeast cells after tranferring to 25°C. Further analysis found that only PMAA_068140 was significantly different expressed according to our previous criteria. PMAA_028730, PMAA_092900, PMAA_032350 PMAA_012920 were more or less variant during dimorphic transition.

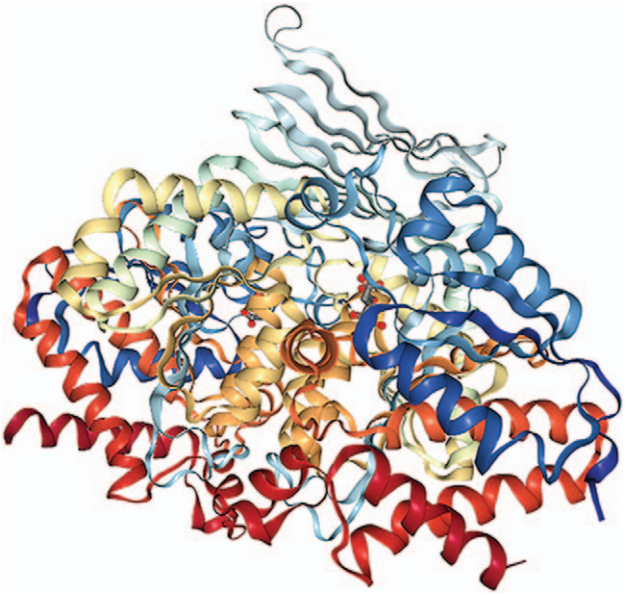

Figure 5. The predicted three-dimensional structure of PMAA-028730.

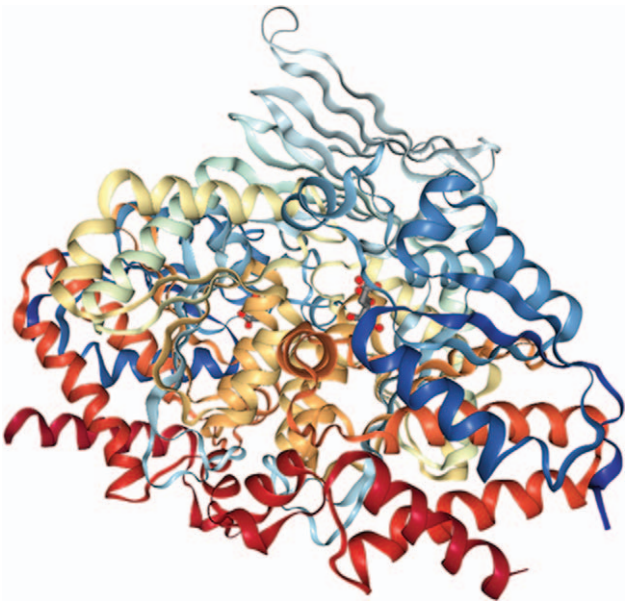

Figure 6. The predicted three-dimensional structure of PMAA-068140.

4. Discussion

T marneffei, mostly prevalent in Southeast Asia, cause deadly systematic infection not only in immunocompromised person, but also in immunocompetent person, resulting from immuno-

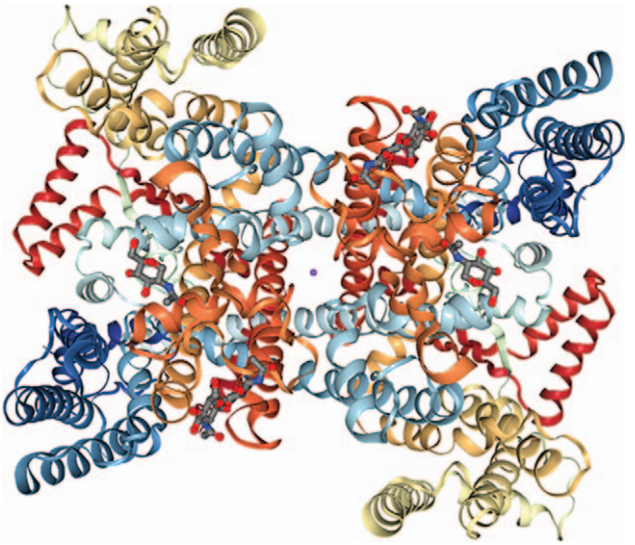

Figure 7. The predicted three-dimensional structure of PMAA-032350.

suppressant abuse. Once infected, it can evolve into a refractory disease. It is widely accepted that this fungus possessed the ability of dimorphic switch. And the yeast form was found in infected individuals and thus represents the pathogenic phase. Therefore, delving the potential molecular mechanism among phase transition stands a good chance to draw forth more precise therapy by molecular target therapy. Though the number of researches focuses on genome, proteome and virulence is growing year by year, there is few researches probing the expression profile difference during dimorphism transition. In present study, the DEGs in dimorphic transition were investigated for the first time and further survey their molecular function.

GO enrichment analysis shown that generation of precursor metabolites and energy was the top one for GO term of BP, and mitochondrion for CC, while oxidoreductase activity occupied the first place of MF in GSM23. This result suggested that the DEGs of conidiation versus hyphal cell types played a vital part in energy metabolism. For GSM24, organic acid metabolic process, isocitrate dehydrogenase activity took the first place for GO term BP and MF respectively, which implied that the two items mentioned above were the potential mechanism in yeast versus hyphal cell types. Also, organic acid metabolic process, membrane and dioxygenase activity were the parallel terms for GSM25. Namely, the DEGs of yeast versus conidiation cell types played a part in organic acid metabolic process, membrane and dioxygenase activity. As for pathway analysis, none of the three platforms yield significant outcome. The leading cause of this phenomenon may be the small number of elected chips, therefore, more experiments are needed to evaluate the DEGs between dimorphic transmission. To sum up, the biological function of DEGs in all the three platforms are mainly concerned with energy metabolism.

STRING functional protein association network was constructed and five genes (PMAA_012920, PMAA_028730, PMAA_068140, PMAA_092900, PMAA_032350) were found showing the strongest connections in all the three platforms surprisingly. Therefore, we have very reason to expect these five genes to be the hub-genes and their features in the switch are indispensable. What's more, from the PPI network, we can obtain the information that the protein structures of those hub-genes remained indefinite. Thus, we predicted the three-dimensional structures of those hub-genes for further understanding of the hub-genes' function. Except for PMAA_092900, significant three-dimensional structures of all the four genes were predicted. When referring to PDB database and PubMed database, the parallel templates for the four hub-genes: PMAA_012920, PMAA_028730, PMAA_068140, PMAA_032350 for constructing their three-dimensional structures were extracted: Crystal structure of Saccharomyces cerevesiae mitochondrial NADP (+)-dependent isocitrate dehydrogenase in complex with isocitrate, major histocompatibility complex (MHC)-independent T-cell receptor B12A, Isocitrate Dehydrogenase (Apo Form), Crystal Structure Of ATP-Dependent Phosphoenolpyruvate Carboxykinase From Thermus thermophilus HB8. Thus, we focus on the function of those templates which may be viewed as the prediction function of the predicted protein structures.

Saccharomyces cerevesiae mitochondrial NADP (+)-dependent isocitrate dehydrogenase (NADP-IDH) in complex with isocitrate Saccharomyces cerevesiae mitochondrial NADP (+)-dependent isocitrate dehydrogenase (NADP-IDH) in complex with isocitrate plays a crucial role in Kreb's cycle and catalyzes oxidative decarboxylation of isocitrate (ICT) into aketoglutarate (AKG). Furthermore, it has been reported that cellular defense against oxidative damage, detoxification of reactive oxygen species, as well as synthesis of fat and cholesterol through generation of NADPH and AKG were other aspects of eukaryotic NADP-IDHs.[10] While a single type of NADP-dependent IDH contributed to most bacteria and archaea (NADP-IDH) for catalyzing reaction during the Krebs cycle, two for eukaryotes, meaning the types of IDHs employ either nicotinamide adenine dinucleotide (NAD) or NADP as a coenzyme, as Peng Y et al reported.[11] In the view of sequence analysis, the NADP-IDHs can be mainly divided into two subfamilies.[12] Subfamily II NADP-IDHs include mainly eukaryotic NADP-IDHs and a few bacterial NADP-IDHs while most bacterial and archaeal NADP-IDHs was part of subfamily I. T marneffei, accepted as a momentous fungus, being part of eukaryon, naturally, possess subfamily II NADP-IDHs and owns two type of IDHs using either NAD or NADP. Regarding to that human belongs to eukaryon as T marneffei, research into the difference of NADP-IDH between T marneffei and human being may provide a target to treat penicilliosis doing no harm to patients.

Organellar two-pore channels (TPCs) Belonging to the voltage-gated ion channel superfamily,[13] function as a homodimer with each subunit containing two homologous Shaker -like 6-TM repeats.[14] TPCs, are associated with various physiological processes in mammalian, such as autophagy regulation,[15] mTOR-dependent nutrient sensing,[16] lipid metabolism[17] and Ebola virus infection. Since TPCs are ubiquitously expressed in animals and plants[18] and TM is subjected to fungus, there was no TPCs in T marneffei. However, based on similar structure, the protein translated by PMAA_028730 may play a similar role as TPCs in fungus, that is, this kind of protein is likely linked with autophagy regulation, mTOR-dependent nutrient sensing, lipid metabolism. Nevertheless, to verify this assumption, more experiments are needed.

Yeast NAD-specific Isocitrate Dehydrogenase controlling a rate-limiting step in the tricarboxylic acid cycle by catalyzing the oxidative decarboxylation of isocitrate to α-ketoglutarate, is a hetero-octamer composed of four IDH1 and four IDH2 subunits, in which, IDH2 functions as catalytic subunit with isocitrate/Mg- and NAD-binding site, while IDH1 functions in cooperative binding of isocitrate and in binding of the allosteric activator AMP. Being consistent with yeast in the respect of microscopic species, T marneffei shares analogous functions with yeast. Thus, we can draw the conclusion that the protein translated by PMAA_068140 may act as a momentous role as NAD-specific isocitrate dehydrogenase in tricarboxylic acid cycle.

Crystal Structure of ATP-Dependent Phosphoenolpyruvate Carboxy kinase From Thermus thermophilus HB8 Phosphoenolpyruvate carboxykinase (PEPCK) isoforms are well known as rate-limiting enzymes for gluconeogenesis and glycerol neogenesis pathways. Montal et al reported that inhibition of phosphoenolpyruvate carboxykinase blocks lactate utilization and impairs tumor growth in colorectal cancer.[19] Thermus thermophilus HB8, an extreme thermophile, has an optimum growth temperature of 348 K (TtPEPCK), which requires a more rigid thermostability. As Sugahara, M et al reported, the intra protomer hydrogen-bond interactions do not account for the thermostability of TtPEPCK while the entropic effects may contribute significantly to the higher stability.[20] Since TM relies on the particular temperature of 25°C or 37°C, while HB8 can withstand the extreme temperature of 348k, this predicted structure may contribute mostly to the thermostability of T marneffei.

All in all, not only in the process of GO function analysis, but also in the three-dimensional structure prediction and further investigation of specific function of each hub-gene, energy metabolism was the common ground for all of the results. Thus, we can conclude that the hub-genes were principal participating in the regulation of energy metabolism.

Still, limitations were found owing to the number of chips and bioinformatics tools elected. We aimed at revealing the secrets in the dimorphism transition, and the datasets eligible for our research was no other than GSE51109 and GSE51110, further researches about the dimorphic transition of T marneffei are calling for.

Author contributions

Conceptualization: Jiemei Cen, Jiarui Chen, Ye Qiu, Jianquan Zhang.
Data curation: Jiemei Cen, Jiarui Chen, Ye Qiu, Jianquan Zhang.
Formal analysis: Jiemei Cen, Jiarui Chen, Wen Zeng, Jianquan Zhang.
Funding acquisition: Jianquan Zhang.
Investigation: Jiemei Cen, Jiarui Chen, Wen Zeng, Jianquan Zhang.
Methodology: Jiemei Cen, Jiarui Chen, Ye Qiu, Wen Zeng, Jianquan Zhang.
Project administration: Jiemei Cen, Jiarui Chen, Jianquan Zhang.
Resources: Jiemei Cen, Jiarui Chen, Jianquan Zhang.
Software: Jiemei Cen, Jiarui Chen, Ye Qiu, Wen Zeng, Jianquan Zhang.
Supervision: Jiemei Cen, Jianquan Zhang.
Validation: Jiemei Cen, Jiarui Chen, Jianquan Zhang.
Visualization: Jiemei Cen, Jiarui Chen, Jianquan Zhang.
Writing – original draft: Jiemei Cen, Jiarui Chen.
Writing – review & editing: Jiemei Cen, Jiarui Chen, Jianquan Zhang.

References

[1] Li Y, Luo H, Fan J, et al. Genomic analysis provides insights into the transmission and pathogenicity of Talaromyces marneffei. Fungal Genet Biol 2019;130:54–61.
[2] Feng J, He L, Xiao X, et al. Methylcitrate cycle gene MCD is essential for the virulence of Talaromyces marneffei. Medical mycology 2020;58:351–61.
[3] Guillaumet-Adkins A, Rodríguez-Esteban G, Mereu E, et al. Single-cell transcriptome conservation in cryopreserved cells and tissues. Genome Biol 2017;18:45.
[4] Dulken BW, Buckley MT, Navarro Negredo P, et al. Single-cell analysis reveals T cell infiltration in old neurogenic niches. Nature 2019;571:205–10.
[5] Dwivedi P, Chutipongtanate S, Muench DE, et al. SWATH-Proteomics of Ibrutinib's Action in Myeloid Leukemia Initiating Mutated G-CSFR Signaling. Proteomics Clin Appl 2020;14:e1900144.
[6] Dwivedi P, Muench DE, Wagner M, et al. Time resolved quantitative phospho-tyrosine analysis reveals Bruton's Tyrosine kinase mediated signaling downstream of the mutated granulocyte-colony stimulating factor receptors. Leukemia 2019;33:75–87.
[7] Samson RA, Yilmaz N, Houbraken J, et al. Phylogeny and nomenclature of the genus Talaromyces and taxa accommodated in Penicillium subgenus Biverticillium. Stud Mycol 2011;70:159–83.
[8] Pasricha S, Payne M, Canovas D, et al. Cell-type-specific transcriptional profiles of the dimorphic pathogen Penicillium marneffei reflect distinct reproductive, morphological, and environmental demands. G3 (Bethesda, Md) 2013;3:1997–2014.
[9] Lau SK, Chow WN, Wong AY, et al. Identification of microRNA-like RNAs in mycelial and yeast phases of the thermal dimorphic fungus Penicillium marneffei. PLoS Negl Trop Dis 2013;7:e2398.
[10] Sugahara M, Ohshima N, Ukita Y, et al. Structure of ATP-dependent phosphoenolpyruvate carboxykinase from Thermus thermophilus HB8 showing the structural basis of induced fit and thermostability. Acta Crystallograph Section D, Biol Crystallogr 2005;61(Pt 11):1500–7.
[11] Peng Y, Zhong C, Huang W, et al. Structural studies of Saccharomyces cerevesiae mitochondrial NADP-dependent isocitrate dehydrogenase in different enzymatic states reveal substantial conformational changes during the catalytic reaction. Protein Sci 2008;17:1542–54.
[12] Margittai E, Banhegyi G. Isocitrate dehydrogenase: A NADPH-generating enzyme in the lumen of the endoplasmic reticulum. Arch Biochem Biophys 2008;471:184–90.
[13] Lau SKP, Lo GCS, Chow FWN, et al. Novel partitivirus enhances virulence of and causes aberrant gene expression in Talaromyces marneffei. mBio 2018;9:
[14] Weerasinghe H, Payne M, Beard S, et al. Organism-wide studies into pathogenicity and morphogenesis in Talaromyces marneffei. Future Microbiol 2016;11:511–26.
[15] Payne M, Weerasinghe H, Tedja I, et al. A unique aspartyl protease gene expansion in Talaromyces marneffei plays a role in growth inside host phagocytes. Virulence 2019;10:277–91.
[16] Woo PC, Lau SK, Lau CC, et al. Penicillium marneffei fungaemia in an allogeneic bone marrow transplant recipient. Bone Marrow Transplant 2005;35:831–3.
[17] Supparatpinyo K, Khamwan C, Baosoung V, et al. Disseminated Penicillium marneffei infection in southeast Asia. Lancet (London, England) 1994;344:110–3.
[18] Vanittanakom N, Cooper CRJr, Fisher MC, et al. Penicillium marneffei infection and recent advances in the epidemiology and molecular biology aspects. Clin Microbiol Rev 2006;19:95–110.
[19] She J, Guo J, Chen Q, et al. Structural insights into the voltage and phospholipid activation of the mammalian TPC1 channel. Nature 2018;556:130–4.
[20] Woo PC, Chong KT, Tse H, et al. Genomic and experimental evidence for a potential sexual cycle in the pathogenic thermal dimorphic fungus Penicillium marneffei. FEBS Lett 2006;580:3409–16.